Novel Foveal Features Associated With Vision Impairment in Multiple Sclerosis

Aubrey Hargrave,[1] Nripun Sredar,[1] Fareshta Khushzad,[1] Jennifer Yarp,[1] Anna Tomczak,[2] May Han,[2] Lucas Kipp,[2] Alfredo Dubra,[1] and Heather E. Moss[1,2]

[1]Department of Ophthalmology, Stanford University, Palo Alto, California, United States
[2]Department of Neurology & Neurological Sciences, Stanford University, Palo Alto, California, United States

Correspondence: Aubrey Hargrave, Department of Ophthalmology, Stanford University, 2370 Watson Court, Palo Alto, CA 94303, USA; aubreych@stanford.edu.

AD and HEM contributed equally to the work presented here and should therefore be regarded as equivalent authors.

Received: May 3, 2021
Accepted: August 23, 2021
Published: September 28, 2021

Citation: Hargrave A, Sredar N, Khushzad F, et al. Novel foveal features associated with vision impairment in multiple sclerosis. *Invest Ophthalmol Vis Sci.* 2021;62(12):27. https://doi.org/10.1167/iovs.62.12.27

Purpose. To characterize scattering and hyperreflective features in the foveal avascular zone of people with multiple sclerosis (MS) using adaptive optics scanning laser ophthalmoscopy (AOSLO) and to evaluate their relationship with visual function and MS disease characteristics.

Methods. Twenty subjects with MS underwent confocal reflectance and non-confocal split-detection AOSLO foveal imaging. Peripapillary retinal nerve fiber layer thickness was measured using optic nerve optical coherence tomography. Blood pressure, intraocular pressure (IOP), and best-corrected high-contrast visual acuity (HCVA) and low-contrast visual acuity (LCVA) were measured. AOSLO images were graded to determine the presence and characteristics of distinct structures.

Results. Two distinct structures were seen in the avascular zone of the foveal pit. Hyperreflective puncta, present in 74% of eyes, were associated with IOP and blood pressure. Scattering features, observed in 58% of eyes, were associated with decreased HCVA and LCVA, as well as increased MS duration and disability, but were not associated with retinal nerve fiber layer thickness. Hyperreflective puncta and scattering features were simultaneously present in 53% of eyes.

Conclusions. Hyperreflective puncta were associated with parameters affecting ophthalmic perfusion, but they were not associated with MS disease parameters. Scattering features were associated with parameters corresponding to advanced MS, suggesting that they may be related to disease progression. Scattering features were also correlated with reduced visual function independent from ganglion cell injury, suggesting the possibility of a novel ganglion cell–independent mechanism of impaired vision in people with MS.

Keywords: adaptive optics scanning laser ophthalmoscopy, multiple sclerosis, fovea

Multiple sclerosis (MS) is the leading cause of neurologic disability in young adults,[1] affecting nearly a million individuals in the United States, and postmortem studies have shown that 90% of people with MS have lesions in their visual pathway.[2] In people with MS, vision-specific quality of life (VS-QOL) is consistently below that of control populations.[3–5] VS-QOL and measures of central visual function, such as low-contrast visual acuity (LCVA), correlate with optical coherence tomography (OCT) measures of retinal ganglion cell (RGC) loss, which is common in people with MS.[6,7] RGCs and their axons progressively deteriorate in MS and sustain acute injury following optic neuritis, a common MS relapse syndrome characterized by vision loss.[8–16] However, neither damage to the optic nerve, including the loss of RGCs and their axons, nor cerebral involvement in MS can account for foveal dysfunction measured using multifocal electroretinography.[17] Additionally, correlation between OCT measures of retinal structure and visual function is weak, suggesting that not all relevant mechanisms of vision loss in MS have been identified.[17,18] This raises the possibility of foveal injury in MS that is not readily detectable with current ophthalmic imaging such as OCT. Therefore, in addition to en face OCT, we examined the fovea of people with MS using reflectance confocal and non-confocal split-detection (multiple-scattering) adaptive optics scanning light ophthalmoscopy (AOSLO).

AOSLO reveals the retina non-invasively, with almost an order of magnitude superior transverse resolution compared with current non-adaptive optics ophthalmoscopes, such as fundus cameras and OCTs. AOSLO has been used to image the photoreceptor mosaic[19–24] and superficial retinal features in many conditions.[25–30] The limited applications of AOSLO to MS have reported foveolar reflective dots in a single subject that were not specific to MS[25] and normal foveal cone photoreceptor densities in three patients with prior optic neuritis and chronic central vision loss.[31] Cone photoreceptor loss visualized with adaptive optics optical coherence tomography (AO-OCT) was also reported in an MS patient who also had other autoimmune diseases.[32] In this work, we report foveal AOSLO imaging of subjects

with relapsing–remitting (RR) and secondary progressive (SP) MS to search for and characterize pathology that might contribute to central vision dysfunction.

Materials and Methods

Subjects

Subjects with RRMS or SPMS were recruited from the Stanford Multiple Sclerosis Center. All subjects met the McDonald criteria for RRMS at some point in their disease course.[33] Additional inclusion criteria for current RRMS subjects included no evidence of disease activity on clinical (i.e., no relapses and no disability progression over 6 months) and radiographic (i.e., no new lesions or enhancing lesions on magnetic resonance imaging) grounds. The RRMS patients who had converted to SPMS were identified using validated criteria.[34] Exclusion criteria included history of optic neuritis in both eyes (one eye was acceptable), neurological disease other than MS and ophthalmic disease other than refractive error, and cataract or optic neuritis more than 1 year prior in one eye. These were assessed based on subject interview and chart review. The research followed the tenets of the Declaration of Helsinki. Informed written consent was obtained from all subjects after explanation of the study goals and possible consequences. The study protocol was approved by the institutional review board at Stanford University School of Medicine.

Subject demographics (age, sex, race/ethnicity) were self-reported, and MS disease parameters were extracted from the medical record. MS disease parameters included phenotype (RR or SP), current and past MS disease-modifying therapies, years since first symptom of MS, and history of optic neuritis in each eye. Disability, classified using the Kurtzke Expanded Disability Status Scale (EDSS)[3] with scores ranging from 0 to 7, was provided by the treating neuro-immunologist. Study testing as described below was performed during one or two visits to the Mary M. and Sash A. Spencer Center for Vision Research at the Byers Eye Institute at Stanford.

Visual Assessment

Intraocular pressure was assessed using a Tono-Pen (Reichert Technologies, Depew, NY, USA). Blood pressure was measured using an automated cuff. Best-corrected high-contrast visual acuity (HCVA) and 2.5% LCVA were measured for each eye using the Early Treatment for Diabetic Retinopathy Study (ETDRS) protocol and Sloan charts.[35]

OCT Imaging

OCT circular B-scans centered on the optic nerve were obtained using a Spectralis OCT (Heidelberg Engineering, Heidelberg, Germany). Retinal ganglion cell atrophy was derived from these scans as the average thickness of the retinal nerve fiber layer (RNFL) around the optic nerve using the manufacturer-supplied analysis software. Additional OCT volumetric scans centered on the fovea were obtained using the Spectralis OCT and the Avanti OCT (Optovue, Inc., Fremont, CA, USA). Finally, multiple horizontal Spectralis OCT B-scans through the foveal center (defined by fixation) were acquired, averaged, and then inspected for evidence of foveal hypoplasia by three raters (AH, AD, HEM) using criteria described in the literature.[36–38] To evaluate inner limiting membrane (ILM) abnormalities, the automatically segmented ILMs in the Avanti OCT foveal volumes were also inspected for segmentation errors (none was found). En face OCT images were constructed with slabs 6 µm above and 15 µm below the ILM. Three raters (AH, AD, HEM) blinded to AOSLO results, reviewed the scans for evidence of superficial retinal abnormalities such as epiretinal membranes.

Ocular Biometry

Axial length (IOLMaster; Carl Zeiss Meditec, Dublin, CA, USA) was obtained in all subjects but one for scaling of AOSLO retinal images.[39] In the only subject where the axial length was not obtained, the average axial length of the 38 eyes was calculated (23.7 µm) and used to scale the retina. This subject had no refractive error.

Adaptive Optics Imaging and Image Analysis

Subjects' pupils were dilated with one drop of 1% tropicamide and one drop of 2.5% phenylephrine ophthalmic drops. Simultaneous confocal and non-confocal split-detection AOSLO image sequences of 150 frames (reflectance, 790-nm wavelength) of both the superficial retina and the photoreceptor layers within the foveal center were acquired. One or more minimally distorted images were subjectively identified in each image sequence and used as a registration template. A minimum of five images per sequence were then registered against the template and averaged to create high signal-to-noise ratio images.[40] These registered images, approximately 1.5 degree of visual angle across, were manually tiled to cover the entire foveal avascular zone (Photoshop; Adobe Inc., San Jose, CA, USA)

Foveal Structure Classification

Review of AOSLO images revealed two types of abnormal structures in the foveal avascular zone—namely, hyperreflective puncta and scattering features. After developing consensus criteria to describe these structures (see Results), three reviewers (AH, AD, HEM) involved in the development of these criteria, along with two others (NS, who has AOSLO experience; LL), independently rated the images of each eye for the presence or absence of these structures. Subsequently, the five reviewers discussed images for which there was less than 80% agreement and reached consensus. Confocal and split-detection inner retina images and confocal photoreceptor images were viewed simultaneously during the rating process. Split-detection images provided the sharpest capillary and scattering feature edges and were subsequently used for tracing structures. Confocal images of the superficial retina were used to corroborate identification of structures. Images of co-localizing darker regions (shadows) on the photoreceptor mosaic were also used to judge the presence of scattering features. The structures were manually counted using Fiji (ImageJ; National Institutes of Health, Bethesda, MD, USA).[41,42] The foveal avascular zone (FAZ) and the scattering features were manually traced on split-detection images of the superficial retina using Fiji, and then binary masks of these traced areas were created in Fiji.[42] The area of the foveal scattering features and FAZ were calculated from these binary masks as the sum of the area of the corresponding pixels (MATLAB; MathWorks, Natick, MA, USA). MATLAB was used to calculate Feret's diameter for each scattering feature from the binary

Investigative Ophthalmology & Visual Science

masks as the distance between the two farthest points on the feature.

Statistical Analysis

The proportion of eyes with each type of structure and the correlation between eyes in each subject were determined. The distribution of each structure within eyes was characterized by number, total area, and fractional FAZ coverage. Pearson's correlation and linear regression were used to compare feature distribution between eyes of the same subject.

Visual outcomes (HCVA, LCVA) were studied as a function of number of each kind of structure using linear generalized estimating equation (GEE) models accounting for intrasubject correlation between eyes. Multiple variable models considered covariates likely to be associated with visual function, including the RNFL, as a measure of ganglion cell atrophy and age. To address the mechanism of vision loss we considered number, total area, and coverage of the foveal scattering features.

The number of foveal structures was studied using negative binomial distribution GEE models accounting for intrasubject correlation between eyes. Associations with demographic parameters, ophthalmic parameters, and MS disease parameters were considered. For this analysis, race was collapsed to white non-Hispanic and non-white non-Hispanic based on the distribution. Medication associations were studied for medications in which ≥20% of subjects had exposure. This is an exploratory analysis due to the large number of possible covariates considered.

These calculations were performed using SPSS Statistics 26 (IBM, Inc., Armonk, NY, USA), with $P \leq 0.05$ as the threshold for statistical significance.

Table 1. Distribution of Subject-Level Characteristics of MS Subjects Who Completed AOSLO Imaging ($n = 20$)

Characteristic	Distribution
Age (y), median (range)	47 (28–74)
Female gender, *n* (%)	16 (80)
Race/ethnicity, *n* (%)	
White, non-Hispanic	14 (70)
White, Hispanic	1 (5)
Asian	4 (20)
Black, non-Hispanic	1 (5)
Past optic neuritis in one eye, *n* (%)	7 (35)
MS phenotype, *n* (%)	
RRMS	13 (65)
SPMS	7 (35)
MS duration (y), median (range)	12 (1–35)
EDSS, median (range)	2 (0–7.5)
Past and present MS modifying therapies, *n* (%)	
1	5 (25)
2	6 (30)
3	4 (20)
4	4 (20)
5	1 (5)
MS modifying therapy (ever; current), *n* (%)	
None	0 (0); 2 (10)
Glatiramer acetate	11 (55); 1 (5)
Interferon	6 (30); 1 (5)
Fingolimod	6 (30); 4 (20)
Dimethyl fumarate	8 (40); 2 (10)
Natalizumab	5 (25); 1 (5)
Rituximab	1 (5); 0 (0)
Ocrelizumab	9 (45); 8 (40)
Alemtuzumab	1 (5); 1 (5)
Arterial pressure (mm Hg), mean (range)	104.2 (88.7–132.7)

Results

Subjects

Twenty participants (13 RRMS, 7 SPMS) were imaged with AOSLO (Table 1). Two additional subjects agreed to participate but did not have a successful AOSLO imaging due to cataract ($n = 1$) and high axial length precluding focusing ($n = 1$). One eye from each of two imaged participants was excluded for poor image quality, leaving 38 eyes for final analysis; of these, seven eyes (18%) had a history of optic neuritis. Ranges for the eyes in the final analysis included the following: HCVA, 63 to 95 letters; LCVA, 1 to 69 letters; peripapillary RNFL, 66 to 132 µm; axial length, 21 to 26 mm; FAZ area, 0.16 to 0.51 mm^2; and IOP, 14 to 32 mm Hg. Both eyes of one subject had continuation of ganglion cell layers in the fovea consistent with subclinical foveal hypoplasia; one of these eyes also had a fragmented FAZ.[36–38] No other subjects had foveal hypoplasia. Nineteen eyes had epiretinal membranes on en face OCT, with none impacting the fovea.

Hyperreflective Puncta

One of the two types of foveal structures identified in this study is microscopic hyperreflective puncta, located in the superficial retina in the center of the fovea (corresponding to the bottom of the foveal pit (Fig. 1). By rater consensus, 28 eyes (74%) had at least one hyperreflective punctum. The presence of these structures is confounded by the foveal reflex in en face OCT images and cross-sectional OCT B-scans (Figs. 1A, 1E), but they appear highly reflective in confocal AOSLO images (Fig. 1B). Hyperreflective puncta do not appear in the corresponding non-confocal AOSLO split-detection images (Fig. 1C) or confocal AOSLO images of the photoreceptor mosaic (Fig. 1D). Similar structures have been previously described in subjects both with and without ophthalmic disease.[25] In some eyes imaged in this study, these hyperreflective puncta appear to form a curvilinear pattern resembling a string of pearls which, to the best of our knowledge, has not been previously described (Fig. 2A). This pattern was not distinguishable from the foveal reflex in OCT images (Figs. 2B, 2C). The hyperreflective puncta measured 1 to 6 µm in diameter and ranged from 0 to 279 puncta per eye, with their distribution skewed toward the lower amount. Among the 18 subjects with both eyes imaged, hyperreflective puncta were seen in both eyes (10 subjects), one eye (six subjects), and neither eye (two subjects). The number of hyperreflective puncta was correlated between eyes within individuals ($r = 0.85$; $P < 0.0005$, linear regression). The number of hyperreflective puncta was not associated with the presence of epiretinal membranes ($P = 0.367$). The subject with subtle foveal hypoplasia in both eyes had hyperreflective puncta in the eye with a normal FAZ. There were no hyperreflective puncta in the eye with a fragmented FAZ.

Scattering Features

The second type of foveal structure is microscopic scattering features, which are textured, irregularly shaped structures visible in confocal AOSLO superficial retinal images of the central fovea (Figs. 3B, 4A, 4D, 4G, 5A, 5C). By rater

Investigative Ophthalmology & Visual Science

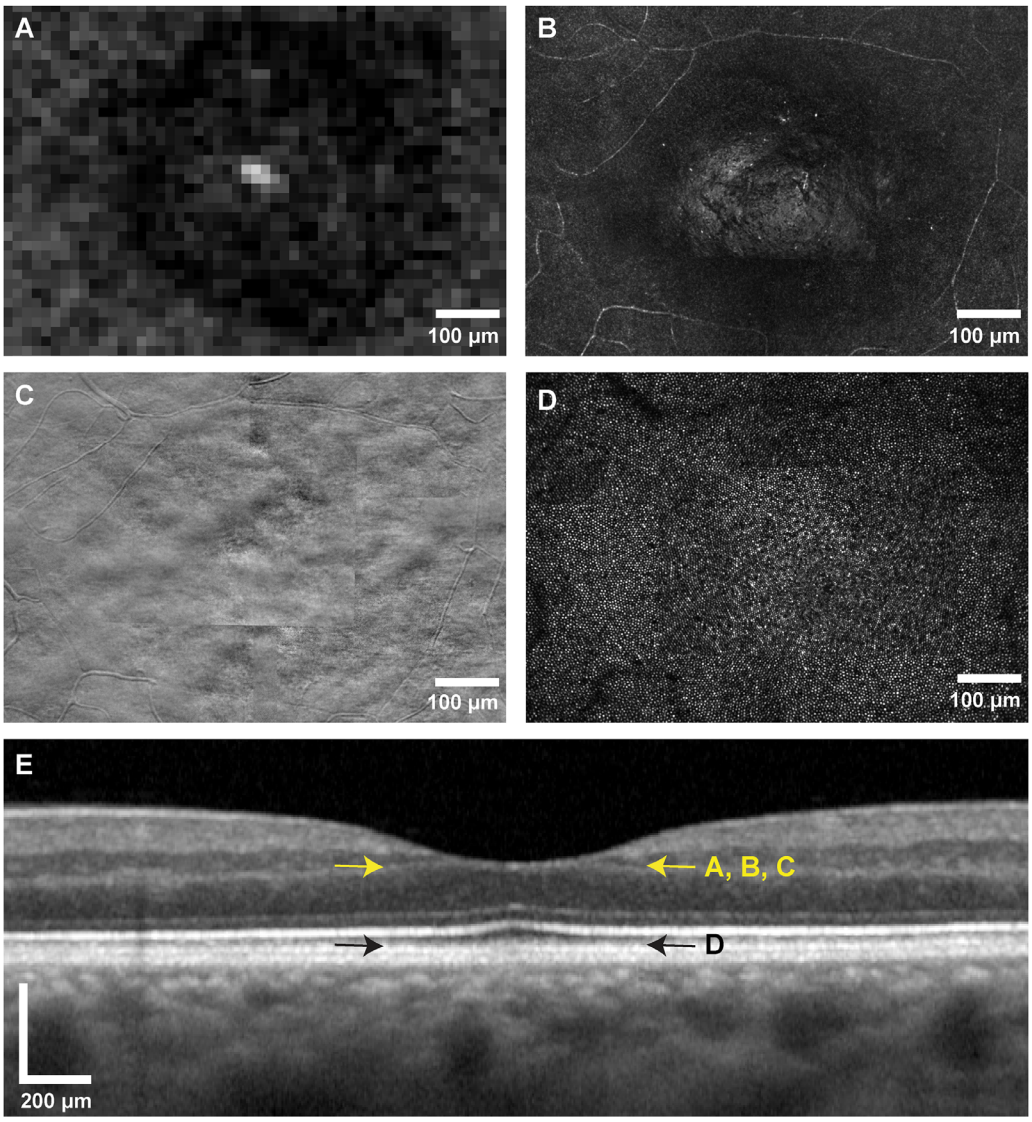

Figure 1. Hyperreflective puncta in the FAZ of people with MS. Hyperreflective puncta, small white reflective structures in the FAZ, are not distinguishable from the foveal reflex in en face OCT images (A), but they are visible in confocal AOSLO images of the superficial retina (B). Hyperreflective puncta are not visible in split-detection AOSLO images of the superficial retina (C), and there are no associated changes on confocal AOSLO images of the corresponding photoreceptor mosaic (D). Hyperreflective puncta are not distinguishable from the foveal reflex in cross-sectional OCT B-scans (E). *Yellow arrows* demarcate the approximate location and size of the superficial retinal images (A–C), and *black arrows* demarcate the approximate location and size of the photoreceptor mosaic (D). *Scale bar:* 100 µm (A–D); 200 µm (E).

consensus, 22 eyes (58%) had scattering features. The well-defined outer borders of the scattering features are visible in non-confocal AOSLO split-detection imaging at the same depth (Figs. 3C, 4B, 4E, 4H, 5B, 5D). Some of these scattering features exhibit circular sections within their borders (Fig. 5B). Although the goal of the study was not to examine the photoreceptors, when viewing the corresponding confocal reflectance AOSLO images of the photoreceptor mosaics we observed co-localizing dark regions with a shape similar to that of the scattering features (Fig. 3D). Of the 22 eyes with scattering features, five eyes had photoreceptor mosaics that were poor image quality or unavailable. Of the remaining 17 eyes, 82% (14 eyes) had correlated dark regions with co-localizing scattering features (1 to 182 scattering features per eye, with total area coverage ranging from 294–81,000 µm^2 per eye), and three eyes did not (two to five scattering features per eye, with total area coverage ranging from 325–15,000 µm^2 per eye). Other than these dark regions, the photoreceptor mosaics were qualitatively normal. The scattering features can be identified in en face OCT images in five out of 22 subjects (23%) in a pattern spatially similar to AOSLO confocal images (Figs. 3A, 4F) but were not distinguishable from the foveal reflex in the remaining subjects (77%) (Figs. 4C, 4I). The scattering features were also not distinguishable from the foveal reflex in OCT B-scans (Fig. 3E). To our knowledge, these scattering features have not been previously described in the literature in MS or any other ophthalmic or neurological disease. The scattering features ranged from 0 to 182 features per eye; their Feret's diameters ranged from 5.3 to 122.6 µm, and their area ranged from 12.9 to 5504 µm^2 per feature (Fig. 5C). This corresponded to a total area of 0 to approximately 81,000 µm^2 per eye, and FAZ coverage of 0.05% to 16.1%. Among 18 subjects with both eyes imaged, scattering

Investigative Ophthalmology & Visual Science

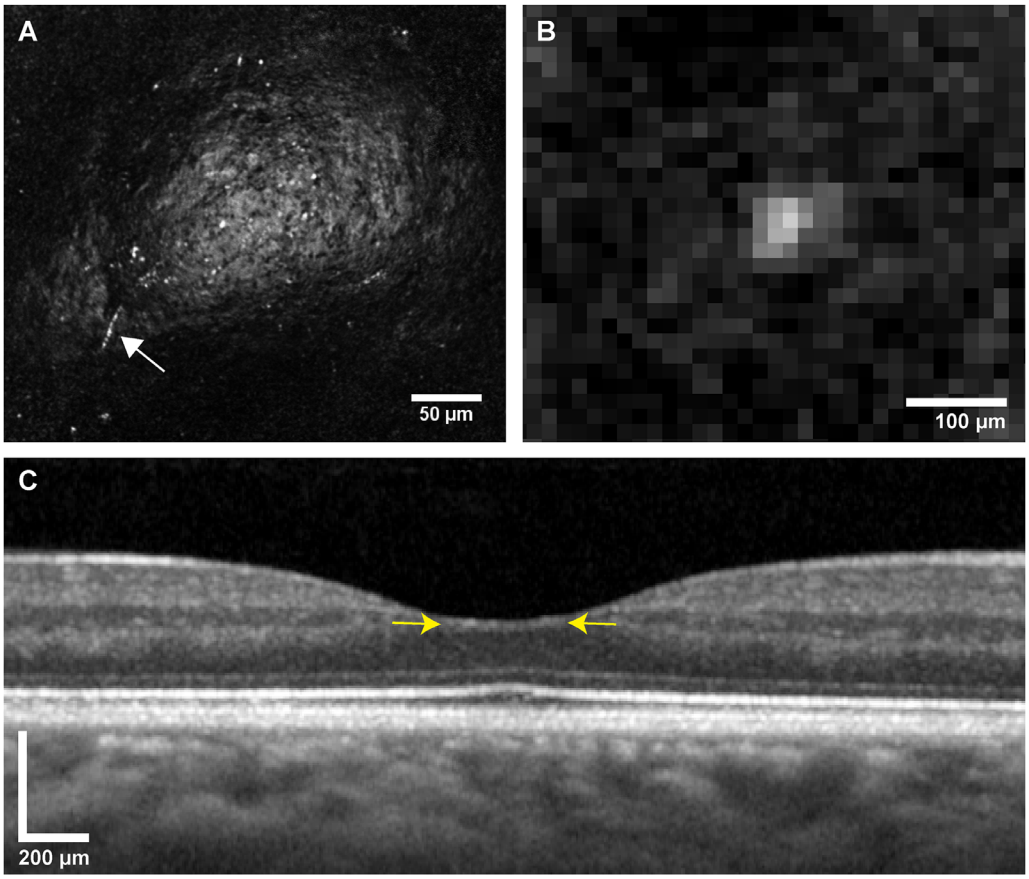

Figure 2. Range of hyperreflective puncta in the foveal pit of a person with MS. (A) Confocal AOSLO image highlights the center of the FAZ of the superficial retina for better visualization of a moderate number of hyperreflective puncta, as well as hyperreflective puncta resembling a string of pearls (*white arrow*). (B) Corresponding en face OCT image of the fovea and foveal reflex and (C) cross-sectional OCT B-scan, where hyperreflective puncta are not distinguishable from the foveal reflex. Yellow arrows are demarcating the approximate location and size of the superficial retinal images (A, B). *Scale bar:* 50 µm (A); 100 µm (B); 200 µm (C).

features were seen in both eyes (six subjects), one eye (eight subjects), and neither eye (four subjects). The number of scattering features was correlated between eyes, although there were prominent outliers ($r = 0.92$; $P < 0.0005$, linear regression). The number of scattering features was also associated with the presence of epiretinal membranes ($P = 0.004$). The subject with subtle foveal hypoplasia had two scattering features in the eye with a normal FAZ and none in the eye with a fragmented FAZ.

Overall, 20 eyes (53%) had both hyperreflective puncta and scattering features (Figs. 4G, 5C), eight eyes had only hyperreflective puncta (21%), two eyes had only scattering features (5%), and eight eyes (21%) had neither. The number of hyperreflective puncta and scattering features were associated ($P < 0.005$, GEE) (Fig. 5F).

Associations Between Microscopic Structures and Vision

HCVA, a measure of visual acuity, was associated with the number of hyperreflective puncta ($P = 0.03$, linear GEE accounting for age, RNFL) (Fig. 6A). Likewise, HCVA was associated with the number of scattering features, the total area of scattering features, and the FAZ coverage of scattering features ($P < 0.0005$, GEE) (Fig. 6B). In unadjusted analysis, HCVA was also associated with age ($P < 0.0005$, GEE) but was not associated with retinal atrophy ($P = 0.13$, GEE, RNFL), FAZ size ($P = 0.06$, GEE), or IOP ($P = 0.48$, GEE). In a multiple variable model, HCVA remained linearly associated with number, total area, and coverage of scattering features ($P < 0.0005$ for all, GEE accounting for age, RNFL). This association persisted in multiple variable models accounting for MS duration. The total area of scattering features was not associated with retinal atrophy ($P = 0.37$, GEE) (Fig. 6C).

LCVA, a measure of visual acuity and contrast sensitivity that has shown promise as a visual outcome measure for MS,[43] was not associated with the number of hyperreflective puncta ($P = 0.38$, GEE accounting for age, RNFL). However, LCVA was linearly associated with number, total area, and coverage of scattering features ($P < 0.0005$, $P = 0.002$, and $P = 0.055$, respectively; GEE) (Fig. 6D). In unadjusted analysis, LCVA was not associated with age ($P = 0.69$, GEE), RNFL ($P = 0.21$, GEE), FAZ size ($P = 0.60$, GEE), or IOP ($P = 0.083$, GEE). In a multiple-variable model, LCVA remained linearly associated with number, total area, and coverage of scattering features ($P < 0.0005$, $P = 0.002$, and $P = 0.019$, respectively; GEE accounting for age, RNFL). This association persisted in multiple variable models accounting for MS duration.

Investigative Ophthalmology & Visual Science

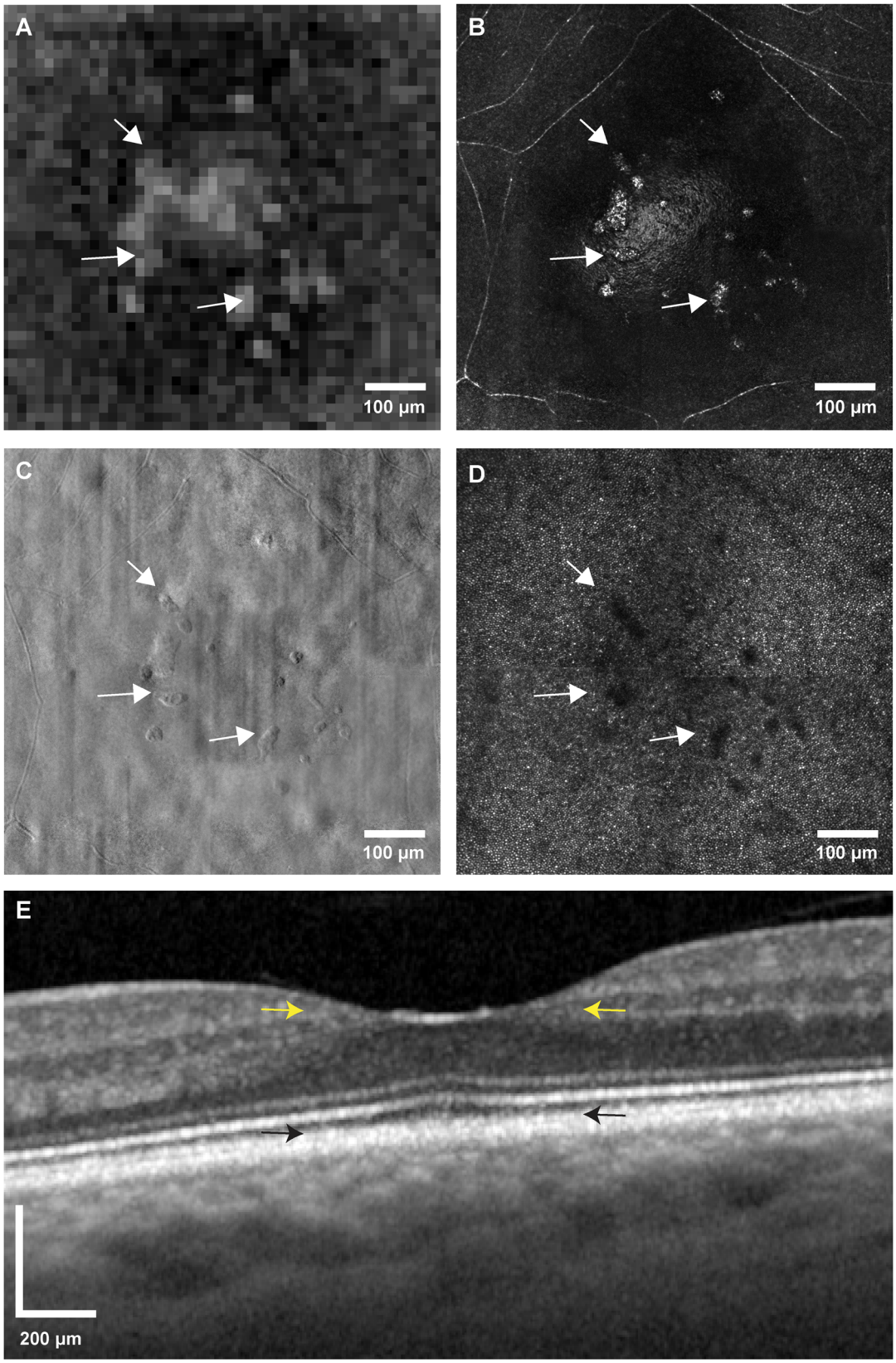

Figure 3. Scattering features in the FAZ of people with MS. *White arrows* highlight examples of scattering features in an en face OCT image of the fovea (A) and a confocal AOSLO image of the superficial FAZ (B). (C) Corresponding split-detection AOSLO image of the superficial retina with scattering features (*white arrows* highlight examples) and (D) corresponding confocal AOSLO image of the photoreceptor mosaic with dark regions (shadows) (*white arrows* highlight examples) that co-localize with the scattering features. (E) Cross-sectional OCT B-scan shows that the scattering features are not distinguishable from the foveal reflex. *Yellow arrows* demarcate the approximate location and size of the superficial retinal images (A–C), and *black arrows* demarcate the approximate size and location of the photoreceptor mosaic (D). *Scale bar:* 100 µm (A–D); 200 µm (E).

Investigative Ophthalmology & Visual Science

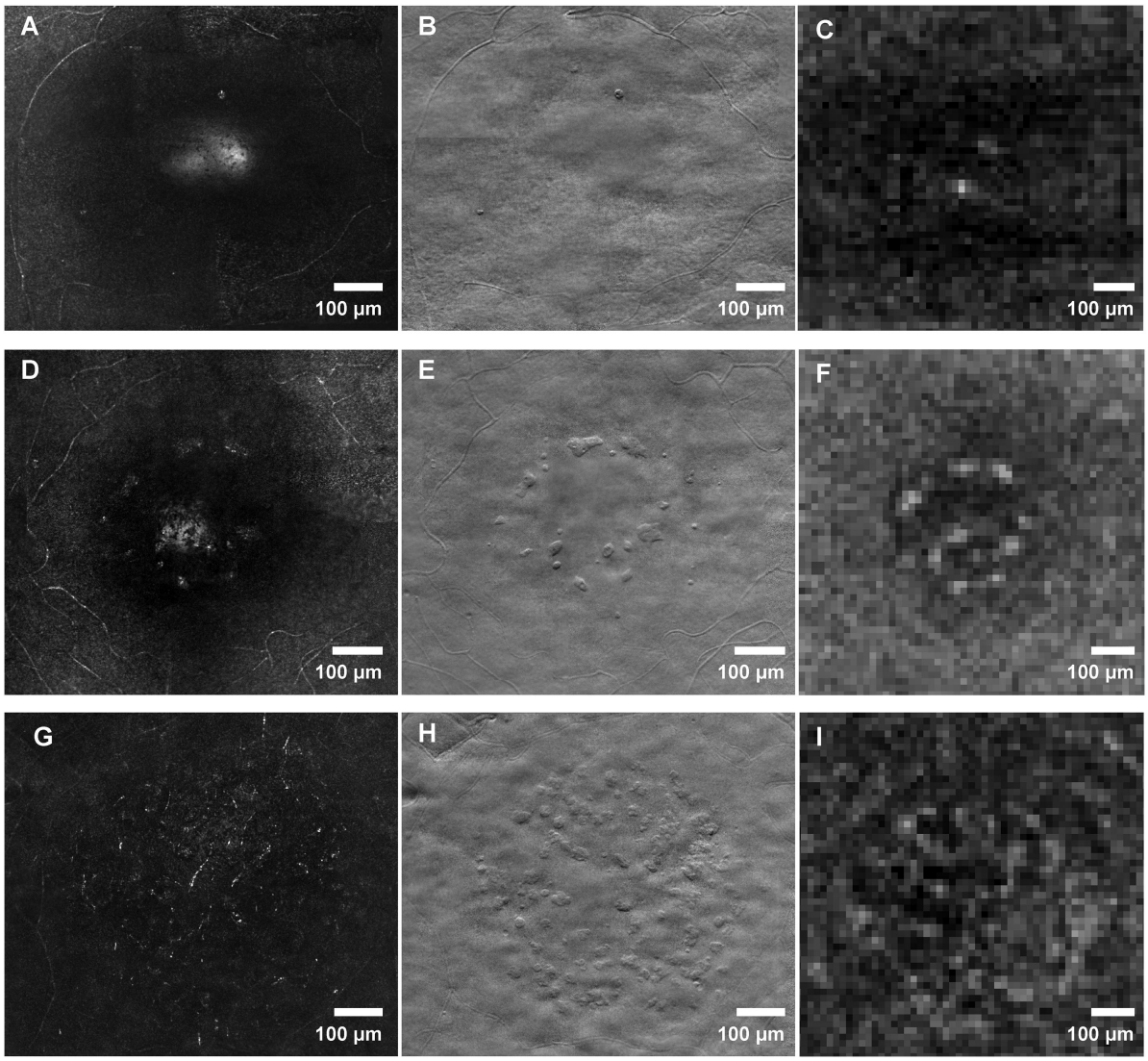

Figure 4. Range of scattering features in the FAZ of people with MS. AOSLO images of the superficial retina of three different eyes show few scattering features (A–C), moderate scattering features (D–F), and many scattering features along with hyperreflective puncta (G–I). The *left column* contains AOSLO confocal images, and the *middle column* contains the corresponding AOSLO split-detection images. The *right column* contains en face OCT images highlighting the fovea. *Scale bar:* 100 µm.

Associations Between Microscopic Structures and MS Disease Characteristics

Exploratory analyses among the number of AOSLO foveal structures and subject demographics, multiple sclerosis disease characteristics, and ophthalmic parameters showed that the number of hyperreflective puncta was not associated with MS duration, severity, current MS treatment, or previous medications (Table 2). Hyperreflective puncta number was also not associated with ganglion cell injury (RNFL thickness) but was associated with IOP, blood pressure, and axial length (Table 2).

The number of scattering features was associated with multiple parameters of advanced MS disease, including age (Table 2, Fig. 7A). Furthermore, the number of scattering features was associated with having been treated with more medications overall (Table 2, Fig. 7B). Scattering features were associated with current ocrelizumab treatment, previous fingolimod treatment, and past or present dimethyl fumarate treatment. Additionally, the number of scattering features was associated with larger FAZ area and the presence of epiretinal membranes, and it was inversely associated with ganglion cell injury. The number of scattering features was not associated with variables impacting ophthalmic perfusion. FAZ area was not associated with measures of MS severity, including duration and disability ($P = 0.32$ and $P = 0.74$, respectively; GEE models accounting for age).[44] In models of number of scattering features accounting for epiretinal membrane presence, the number of scattering features remained associated with MS duration ($P < 0.0005$) and disability (EDSS, $P = 0.02$).

Discussion

We showed the presence of two types of superficial retinal structures in people with MS, which we term hyperreflective puncta and scattering features. To the best of our knowledge, this study is the first to assess foveal superficial retinal

Investigative Ophthalmology & Visual Science

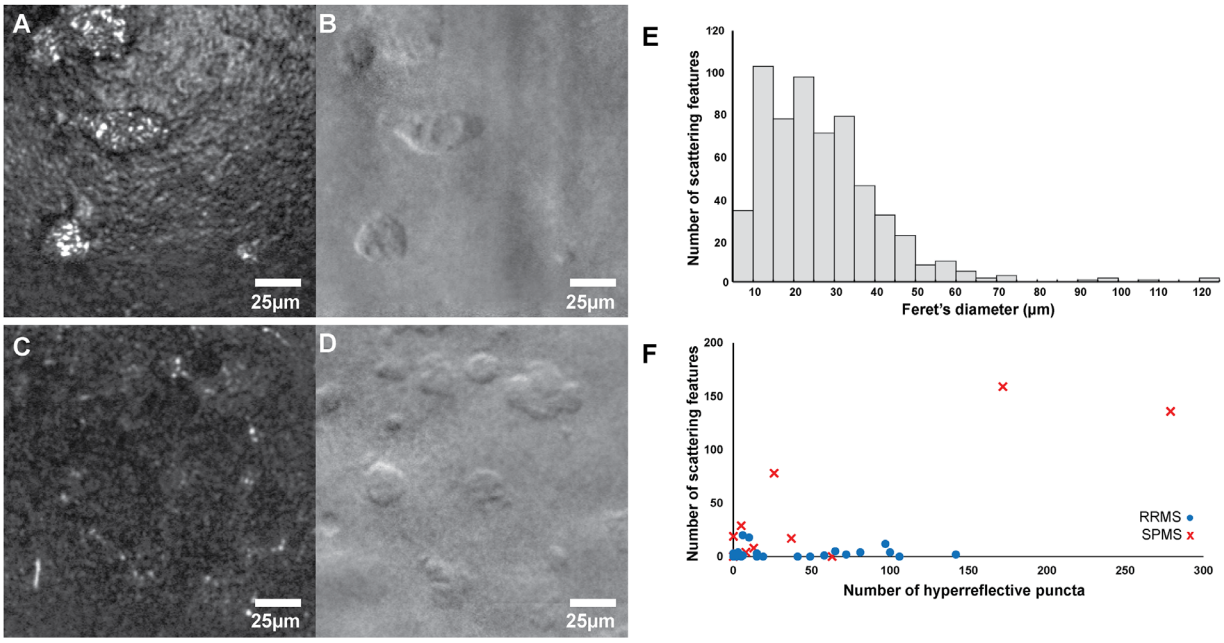

Figure 5. Shape and size distribution of the scattering features. (A) Confocal and (B) split-detection AOSLO superficial retina images of large scattering features show inner structural detail. (C) Confocal and (D) split-detection AOSLO superficial retina images show smaller, clustered scattering features. Hyperreflective puncta are also seen in (C). *Scale bar:* 25 µm. (E) Histogram shows size distribution (Feret's diameter, in µm) of the scattering features across all eyes. (F) Distribution and relationship between number of scattering features and number of hyperreflective puncta. Each *marker* represents one eye, and the *marker symbol* indicates MS phenotype, either RRMS (*circle*) or SPMS (*cross*).

changes correlating with visual impairment in these subjects using AOSLO imaging.

The hyperreflective puncta have been previously reported in subjects both with and without neurological and ophthalmic disease using AOSLO imaging. Scoles et al.[25] found "punctate reflective structures" that measured 3 to 5 µm in diameter (n = 51). We found the hyperreflective puncta in our study to have a similar size. We did not find an association between hyperreflective puncta number and MS disease characteristics, supporting the hypothesis of previous investigators that these hyperreflective puncta are not a consequence of disease. Scoles et al.[25] reported that punctate reflectivity lining the superficial surface of the foveal pit was more common in normal subjects over 30 years of age. We did not find an association between hyperreflective puncta number and increasing age, although our youngest subject was 28 years. Overall, these data suggest that we are likely observing the same features that have been described in the literature. Interestingly, we did see associations between hyperreflective puncta and ophthalmic parameters (IOP, mean arterial pressure, and axial length) that hint at a possible contribution of the local ophthalmic environment. Although not unique to MS, vascular disease is known to be associated with worse MS outcomes.[45] Because hyperreflective puncta are correlated with perfusion and blood pressure, they may be an imaging biomarker for vascular risk factors, the modification of which may modulate MS disease activity.

Scoles et al.[25] also observed hyperreflective puncta in and near structural lesions on the inner surface of the retina or just deep in the ganglion cell layer in subjects with rubella retinopathy and achromatopsia. We observed the puncta to be spatially adjacent to the scattering features in our subjects; only two eyes with scattering features lacked puncta (5%), whereas eight eyes with puncta lacked scattering features (21%), suggesting that the presence of puncta might precede scattering features. Interestingly, Scoles et al.[25] noted that the puncta they observed in normal subjects did not shift noticeably over 18 months, but the puncta associated with other structural lesions did change location. This observation deserves future study, particularly in the MS subjects that have both hyperreflective puncta and scattering features.

To our knowledge, we are the first to report the presence of scattering features at the level of the superficial retina in the FAZ of people with MS or any other disease. These textured features are visible in both reflectance confocal and split-detection AOSLO images and are visible in approximately 23% of en face OCT images; consequently, we were not able to predict the presence of scattering features in AOSLO images based on the en face OCT images or vice versa. Scattering features are associated with several markers of advanced MS disease including disability, advanced disease phenotype (SPMS), exposure to more MS disease-modifying therapies, and longer disease duration. Because age is tightly correlated with MS progression, its association with scattering features can also be considered to support these features as markers of advancing MS, although a study including age-matched healthy controls is needed to confirm this observation. Although a medication effect is possible, we believe that the association between the number of scattering features and ocrelizumab is due to this medication being utilized in people with more advanced disease. The negative association between scattering features and fingolimod exposure is interesting, as this class of medications (S1P inhibitors) has clinical effects on the macula, including thickening and in some cases cystoid macular edema.[46] Interestingly, the number of scattering features is

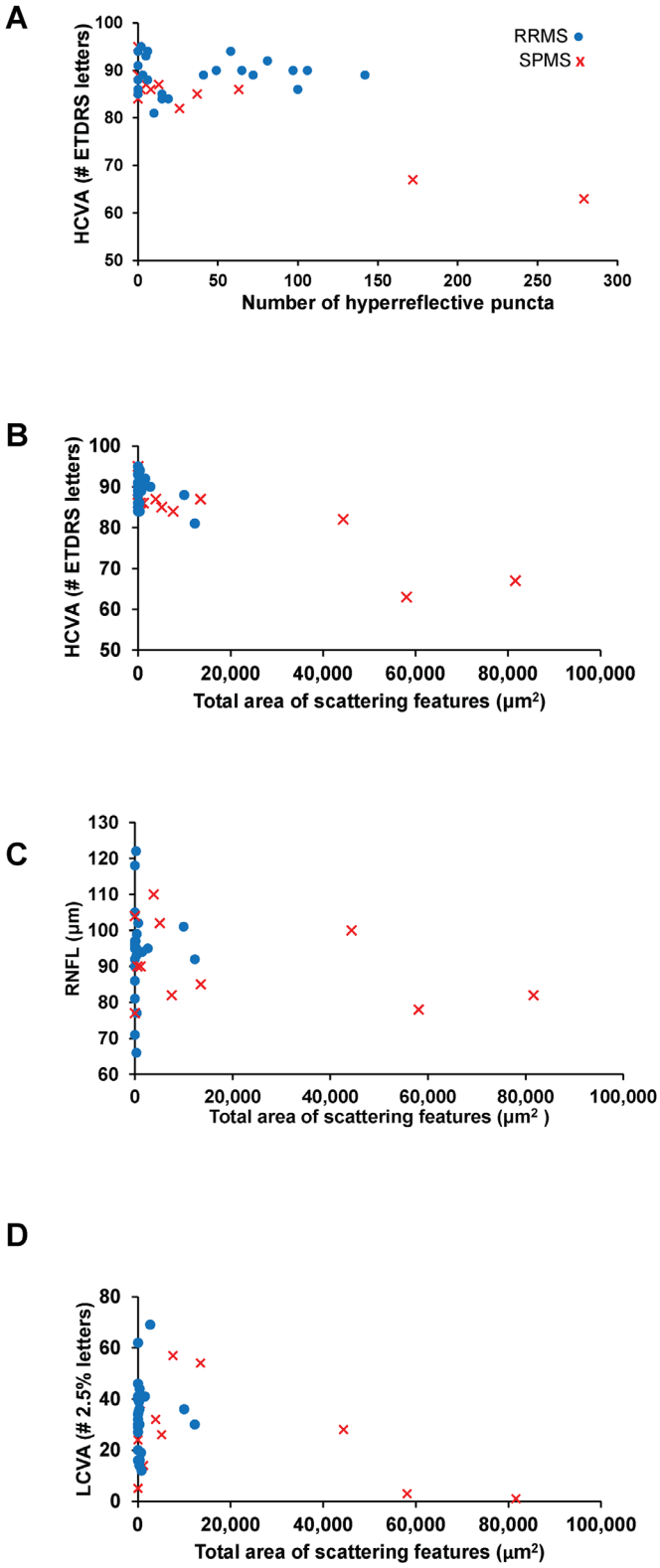

Figure 6. Relationship between AOSLO FAZ features and vision in people with MS. (A) Number of hyperreflective puncta compared with HCVA (ETDRS, number of letters seen). (B) Total area of scattering features (µm^2) compared with HCVA (ETDRS, number of letters seen). (C) Total area of scattering features (µm^2) compared with peripapillary RNFL thickness (µm), a measure of ganglion cell atrophy. (D) Total area of scattering features (µm^2) compared with LCVA (number of 2.5% contrast letters seen). Each marker represents a single eye. Marker style represents the MS phenotype of the subject, either RRMS (*circle*) or SPMS (*cross*).

Investigative Ophthalmology & Visual Science

Table 2. Association Among Number of Features, Subject, and Eye Variables (Negative Binomial GEE Models Accounting for Within-Subject Correlation Between Eyes)

	Hyperreflective Feature Number (*P*)	Scattering Feature Number (*P*)
Demographics		
Older age*	0.12	<0.0005
Female gender	0.535	<0.0005
Non-white, non-Hispanic race	<0.0005	0.14
Multiple sclerosis		
Longer MS duration*	0.53	<0.0005
Higher disability*	0.99	0.001
SPMS phenotype	0.59	<0.0005
MS medication exposure (number)	0.80	<0.0005
Current medication		
Not fingolimod	0.77	<0.0005
Ocrelizumab	0.30	0.0002
Medication exposure		
Not glatiramer	0.47	0.007
Interferon	0.17	0.69
Fingolimod	0.30	0.14
Dimethyl fumarate	0.98	0.001
Natalizumab	0.39	0.087
Ocrelizumab	0.50	0.004
Ophthalmic		
Lack of optic neuritis	0.77	0.003
Thicker RNFL*	0.21	0.046
Bigger FAZ area*	0.49	<0.0005
Epiretinal membrane	0.37	0.004
Higher IOP*	0.027	0.007
Axial length*	0.011	0.51
Higher mean arterial pressure*	<0.0005	0.23

*Indicates variables that were modeled as continuous; all other variables were modeled as dichotomous.

inversely associated with markers of ganglion cell injury in MS, including RNFL thinning and optic neuritis. This finding is unexpected based on other associations we found with markers of advanced disease. This inverse association raises the possibility that the basis of scattering features may be related to a lack of atrophy of ganglion cells, possibly through cause or effect. One possible explanation for the association between both number and area of scattering features and the size of the FAZ is that the density of scattering features in the FAZ is comparable across subjects. However, coverage is also associated with FAZ size, suggesting another possible mechanism in driving development or lack of clearance of these features. Interestingly, FAZ size was not associated with markers of advanced MS.

Importantly, the number and area of the scattering features were correlated with a decrease in visual acuity, as measured by both HCVA and LCVA. This correlation persisted after accounting for age, RNFL thinning, and MS duration. These relationships, along with the lack of a correlation between the presence of scattering features and RNFL thinning, suggest that changes in visual acuity are independent from the visual changes associated with ganglion cell loss that are well described in MS. Teasing out the relative contributions of ganglion cell injury and scattering features will require larger sample sizes. Although it is possible that the presence of the features is a marker for visual pathway injury mediating the vision loss, we find evidence for a causal relationship in our results. The scattering features often co-localize with dark regions in the photoreceptor mosaic, suggesting that the scattering features can cast shadows on the photoreceptors. This phenomenon is similar to the shadow cast by retinal blood vessels, which microperimetry has shown to be associated with decreased retinal sensitivity.[47] This leads us to hypothesize that these shadows may be impacting vision in this critical part of the retina. Given that 1 degree of visual angle corresponds to approximately 300 µm on the retina, a 20/20 letter (5′ arc) projects on 25 µm of retina with details projecting on 5 µm of retina.[48] Thus, the smallest scattering features are sufficient to block part of a 20/20 letter, and the largest can block multiple 20/20 letters. Simulated microscotoma work has shown that random 2.5-µm microscotomas occupying >50% of a 20/20 letter reduce correct identification below 75%.[49] However, larger microscotomas of the sizes corresponding to the scattering features have not been studied to date. The threshold for single scotomas impeding reading corresponds to the size of a saccade.[50] For our BCVA task, we would expect this threshold to be about one letter, which is less than the size of the smallest scattering feature. Interrogating of focal visual thresholds using AO microperimetry would allow investigation of this hypothesis.[51] Because we did not record fixation, we are unable to assess the normality of the cone distribution at the subjects' fixation location,[52,53] but this could be an important area of future research. However, it is interesting to note that the scattering features were not preferentially located in the central fovea but rather were spread throughout the FAZ.

The cross-sectional AOSLO imaging in this study did not allow us to test whether the discovered structures are living cells or inanimate deposits. Both occur in the FAZ, where cellular constituents are limited to photoreceptors and Müller microglia,[54] except in one subject who had subclinical foveal hypoplasia.[36–38] Consequently, the hyperreflective puncta, which do not appear to be specific to

Investigative Ophthalmology & Visual Science

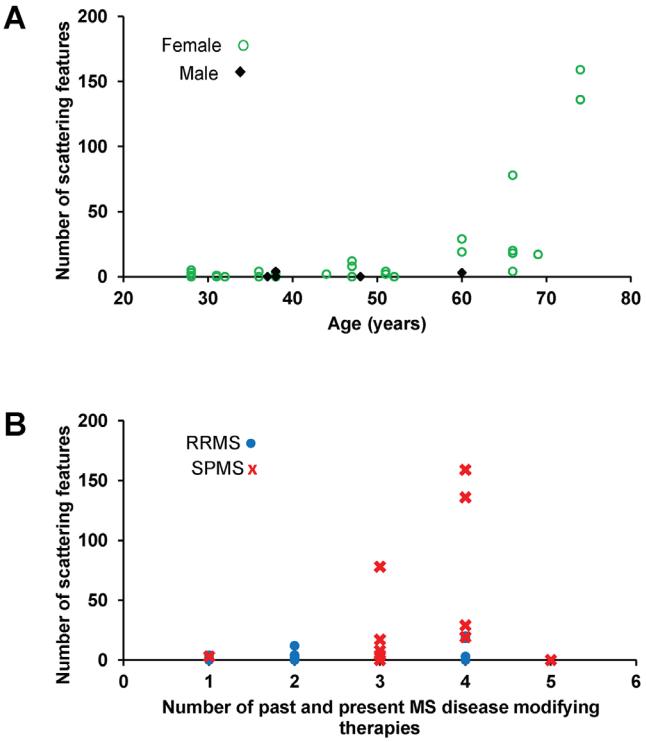

Figure 7. Relationship among scattering features, MS, and demographic parameters. (A) Subject age compared with number of scattering features. Each *marker* represents one eye. *Marker symbol* indicates subject gender, either female (*circle*) or male (*diamond*). (B) Number of past or present MS medications (disease-modifying therapies) compared with the number of scattering features. Each marker represents one eye. The *marker symbol* indicates the MS phenotype, either RRMS (*circle*) or SPMS (*cross*).

MS, have been hypothesized to be Müller cell endfeet,[55] as these are present at the superficial retina, or melanin granules.[25] On the other hand, the scattering features may relate to inflammation or degeneration in MS. One possibility is that the scattering features are microglia, which contribute to homeostasis in the healthy retina but can also respond to pathological conditions.[56] The retina also has a population of resident CD11b+ dendritic cells that can become activated under inflammatory conditions and may migrate to the FAZ.[57] Another possibility is immune cells that infiltrate the tissue during neuroinflammatory conditions.[58] For example, Castanos et al.[59] recently imaged hyaloctyes, the resident macrophages of the vitreous, on the surface of the ILM using OCT. Hyalocytes have been described to have roles in retinal pathology.[60,61] However, as previously described, the scattering features are irregularly shaped, some with internal circular substructures along with extending processes, but they do not have classic dendriform morphology. Possibilities for inanimate deposits may be damage resulting from inflammation, as inflammation in the retina has been shown to result in phagocytosing microglia along with swollen and degenerating neurites in Henle's fiber layer, which is the approximate location of the abnormal structures in our AOSLO superficial retinal images.[62] Longitudinal imaging will aid in making the distinction between cellular and inanimate structure composition. If the features are living cells brought to the foveal pit due to a perturbed microenvironment or are resident microglia, we would expect them to shift their location and morphology over the course of time. Ex vivo work including immunohistochemistry also offers promise for elucidating the composition of the structures.

Our study has several limitations, including the sample size, which limited the extent of statistical associations, particularly the number of variables, that could be considered simultaneously in multiple-variable models. Additionally, as our study did not have healthy controls, it is difficult to draw conclusions about the age-related findings.

In summary, we report microscopic foveal structural changes in the superficial retina of people with MS. Hyperreflective puncta do not appear to be specific to MS. Their number was associated with parameters related to ophthalmic perfusion but was not associated with MS disease parameters. Scattering features in the fovea, however, were associated with parameters corresponding to more advanced MS disease, suggesting that they may be related to MS progression. Interestingly, the scattering features were not associated with ganglion cell atrophy but were associated with visual function, suggesting a ganglion cell–independent role in decreased vision in people with MS.

Acknowledgments

The authors thank Lakshmi Leishangthem for her help with grading images, Bartek Kowalski for the AOSLO image acquisition software, and Moataz Razeen for his technical expertise and helpful discussion.

Supported by the Myelin Repair Foundation; grants from the National Institutes of Health (P30 226877, R01 EY031360, T32 EY027816, R01 EY025231, and EY028287); and an unrestricted grant from Research to Prevent Blindness to the Stanford Department of Ophthalmology.

Disclosure: **A. Hargrave**, None; **N. Sredar**, None; **F. Khushzad**, None; **J. Yarp**, None; **A. Tomczak**, None; **M. Han**, None; **L. Kipp**, None; **A. Dubra**, None; **H.E. Moss**, None

References

1. Bitirgen G, Akpinar Z, Malik RA, Ozkagnici A. Use of corneal confocal microscopy to detect corneal nerve loss and increased dendritic cells in patients with multiple sclerosis. *JAMA Ophthalmol*. 2017;135:777–782.
2. Wallin MT, Culpepper WJ, Campbell JD, et al. The prevalence of MS in the United States: a population-based estimate using health claims data. *Neurology*. 2019;92:e1029–e1040.
3. Kurtzke JF. Rating neurologic impairment in multiple sclerosis: an Expanded Disability Status Scale (EDSS). *Neurology*. 1983;33:1444–1452.
4. Balcer LJ, Baier ML, Kunkle AM, et al. Self-reported visual dysfunction in multiple sclerosis: results from the 25-Item National Eye Institute Visual Function Questionnaire (VFQ-25). *Mult Scler*. 2000;6:382–385.
5. Ma SL, Shea JA, Galetta SL, et al. Self-reported visual dysfunction in multiple sclerosis: new data from the VFQ-25 and development of an MS-specific vision questionnaire. *Am J Ophthalmol*. 2002;133:686–692.
6. Walter SD, Ishikawa H, Galetta KM, et al. Ganglion cell loss in relation to visual disability in multiple sclerosis. *Ophthalmology*. 2012;119:1250–1257.
7. Fisher JB, Jacobs DA, Markowitz CE, et al. Relation of visual function to retinal nerve fiber layer thickness in multiple sclerosis. *Ophthalmology*. 2006;113:324–332.

8. Talman LS, Bisker ER, Sackel DJ, et al. Longitudinal study of vision and retinal nerve fiber layer thickness in multiple sclerosis. *Ann Neurol*. 2010;67:749–760.
9. Graham EM, Francis DA, Sanders MD, Rudge P. Ocular inflammatory changes in established multiple sclerosis. *J Neurol Neurosurg Psychiatry*. 1989;52:1360–1363.
10. Klistorner A, Graham EC, Yiannikas C, et al. Progression of retinal ganglion cell loss in multiple sclerosis is associated with new lesions in the optic radiations. *Eur J Neurol*. 2017;24:1392–1398.
11. Lassmann H. Axonal and neuronal pathology in multiple sclerosis: what have we learnt from animal models. *Exp Neurol*. 2010;225:2–8.
12. Jin J, Smith MD, Kersbergen CJ, et al. Glial pathology and retinal neurotoxicity in the anterior visual pathway in experimental autoimmune encephalomyelitis. *Acta Neuropathol Commun*. 2019;7:125.
13. Alonso R, Gonzalez-Moron D, Garcea O. Optical coherence tomography as a biomarker of neurodegeneration in multiple sclerosis: a review. *Mult Scler Relat Disord*. 2018;22:77–82.
14. Bjartmar C, Wujek JR, Trapp BD. Axonal loss in the pathology of MS: consequences for understanding the progressive phase of the disease. *J Neurol Sci*. 2003;206:165–171.
15. Britze J, Pihl-Jensen G, Frederiksen JL. Retinal ganglion cell analysis in multiple sclerosis and optic neuritis: a systematic review and meta-analysis. *J Neurol*. 2017;264:1837–1853.
16. Green AJ, McQuaid S, Hauser SL, Allen IV, Lyness R. Ocular pathology in multiple sclerosis: retinal atrophy and inflammation irrespective of disease duration. *Brain*. 2010;133:1591–1601.
17. Hanson JVM, Hediger M, Manogaran P, et al. Outer retinal dysfunction in the absence of structural abnormalities in multiple sclerosis. *Invest Ophthalmol Vis Sci*. 2018;59:549–560.
18. You Y, Graham EC, Shen T, et al. Progressive inner nuclear layer dysfunction in non-optic neuritis eyes in MS. *Neurol Neuroimmunol Neuroinflamm*. 2018;5:e427.
19. Qin J, Rinella N, Zhang Q, et al. OCT angiography and cone photoreceptor imaging in geographic atrophy. *Invest Ophthalmol Vis Sci*. 2018;59:5985–5992.
20. Litts KM, Cooper RF, Duncan JL, Carroll J. Photoreceptor-based biomarkers in AOSLO retinal imaging. *Invest Ophthalmol Vis Sci*. 2017;58:BIO255–BIO267.
21. Sun LW, Johnson RD, Williams V, et al. Multimodal imaging of photoreceptor structure in choroideremia. *PLoS One*. 2016;11:e0167526.
22. Georgiou M, Kalitzeos A, Patterson EJ, Dubra A, Carroll J, Michaelides M. Adaptive optics imaging of inherited retinal diseases. *Br J Ophthalmol*. 2018;102:1028–1035.
23. Nesper PL, Scarinci F, Fawzi AA. Adaptive optics reveals photoreceptor abnormalities in diabetic macular ischemia. *PLoS One*. 2017;12:e0169926.
24. Braza ME, Young J, Hammeke TA, et al. Assessing photoreceptor structure in patients with traumatic head injury. *BMJ Open Ophthalmol*. 2018;3:e000104.
25. Scoles D, Higgins BP, Cooper RF, et al. Microscopic inner retinal hyper-reflective phenotypes in retinal and neurologic disease. *Invest Ophthalmol Vis Sci*. 2014;55:4015–4029.
26. Gocho K, Kikuchi S, Kabuto T, et al. High-resolution en face images of microcystic macular edema in patients with autosomal dominant optic atrophy. *Biomed Res Int*. 2013;2013:676803.
27. Huang G, Qi X, Chui TY, Zhong Z, Burns SA. A clinical planning module for adaptive optics SLO imaging. *Optom Vis Sci*. 2012;89:593–601.
28. Takayama K, Ooto S, Hangai M, et al. High-resolution imaging of retinal nerve fiber bundles in glaucoma using adaptive optics scanning laser ophthalmoscopy. *Am J Ophthalmol*. 2013;155:870–881.
29. Takayama K, Ooto S, Hangai M, et al. High-resolution imaging of the retinal nerve fiber layer in normal eyes using adaptive optics scanning laser ophthalmoscopy. *PLoS One*. 2012;7:e33158.
30. Lombardo M, Scarinci F, Ripandelli G, Cupo G, Stirpe M, Serrao S. Adaptive optics imaging of idiopathic epiretinal membranes. *Ophthalmology*. 2013;120:1508–1509.e1.
31. Cuneo A, Zayit-Soudry S, Songster C, et al. High-resolution assessment of cone photoreceptor structure in patients with multiple sclerosis. *Invest Ophthalmol Vis Sci*. 2014;55:1589–1589.
32. Werner JS, Keltner JL, Zawadzki RJ, Choi SS. Outer retinal abnormalities associated with inner retinal pathology in nonglaucomatous and glaucomatous optic neuropathies. *Eye (Lond)*. 2011;25:279–289.
33. Thompson AJ, Banwell BL, Barkhof F, et al. Diagnosis of multiple sclerosis: 2017 revisions of the McDonald criteria. *Lancet Neurol*. 2018;17:162–173.
34. Lorscheider J, Buzzard K, Jokubaitis V, et al. Defining secondary progressive multiple sclerosis. *Brain*. 2016;139:2395–2405.
35. Early Treatment Diabetic Retinopathy Study design and baseline patient characteristics. ETDRS report number 7. *Ophthalmology*. 1991;98:741–756.
36. Linderman RE, Cava JA, Salmon AE, et al. Visual acuity and foveal structure in eyes with fragmented foveal avascular zones. *Ophthalmol Retina*. 2020;4:535–544.
37. Sundaram V, Wilde C, Aboshiha J, et al. Retinal structure and function in achromatopsia: implications for gene therapy. *Ophthalmology*. 2014;121:234–245.
38. Kondo H. Foveal hypoplasia and optical coherence tomographic imaging. *Taiwan J Ophthalmol*. 2018;8:181–188.
39. Litts KM, Georgiou M, Langlo CS, et al. Interocular symmetry of foveal cone topography in congenital achromatopsia. *Curr Eye Res*. 2020;45:1257–1264.
40. Dubra A. HZ. Registration of 2D images from fast scanning ophthalmic instruments. In: Fischer B, Dawant BM, Lorenz C, eds. *Biomedical Image Registration*. Berlin: Springer; 2010:60–71.
41. Schneider CA, Rasband WS, Eliceiri KW. NIH Image to ImageJ: 25 years of image analysis. *Nat Methods*. 2012;9:671–675.
42. Schindelin J, Arganda-Carreras I, Frise E, et al. Fiji: an open-source platform for biological-image analysis. *Nat Methods*. 2012;9:676–682.
43. Balcer LJ, Raynowska J, Nolan R, et al. Validity of low-contrast letter acuity as a visual performance outcome measure for multiple sclerosis. *Mult Scler*. 2017;23:734–747.
44. Gómez-Ulla F, Cutrin P, Santos P, et al. Age and gender influence on foveal avascular zone in healthy eyes. *Exp Eye Res*. 2019;189:107856.
45. Geraldes R, Esiri MM, Perera R, et al. Vascular disease and multiple sclerosis: a post-mortem study exploring their relationships. *Brain*. 2020;143:2998–3012.
46. Moss HE. Visual consequences of medications for multiple sclerosis: the good, the bad, the ugly, and the unknown. *Eye Brain*. 2017;9:13–21.
47. Tuten WS, Tiruveedhula P, Roorda A. Adaptive optics scanning laser ophthalmoscope-based microperimetry. *Optom Vis Sci*. 2012;89:563–574.
48. Smith G, Atchison D. *The Eye and Visual Optical Instruments*. Cambridge, UK: Cambridge University Press; 1997.
49. Seiple W, Holopigian K, Szlyk JP, Greenstein VC. The effects of random element loss on letter identification: implications for visual acuity loss in patients with retinitis pigmentosa. *Vision Res*. 1995;35:2057–2066.

Investigative Ophthalmology & Visual Science

50. Anne-Catherine Scherlen VG. The difference between mean saccade size and scotoma size is a predictive factor for reading speed. *Int Congress Ser*. 2005;1282:704–708.
51. Foote KG, De la Huerta I, Gustafson K, et al. Cone spacing correlates with retinal thickness and microperimetry in patients with inherited retinal degenerations. *Invest Ophthalmol Vis Sci*. 2019;60:1234–1243.
52. Putnam NM, Hofer HJ, Doble N, Chen L, Carroll J, Williams DR. The locus of fixation and the foveal cone mosaic. *J Vis*. 2005;5:632–639.
53. Wilk MA, Dubis AM, Cooper RF, Summerfelt P, Dubra A, Carroll J. Assessing the spatial relationship between fixation and foveal specializations. *Vision Res*. 2017;132: 53–61.
54. Yamada E. Some structural features of the fovea centralis in the human retina. *Arch Ophthalmol*. 1969;82:151–159.
55. Delaunay K, Khamsy L, Kowalczuk L, et al. Glial cells of the human fovea. *Mol Vis*. 2020;26:235–245.
56. Singaravelu J, Zhao L, Fariss RN, Nork TM, Wong WT. Microglia in the primate macula: specializations in microglial distribution and morphology with retinal position and with aging. *Brain Struct Funct*. 2017;222:2759–2771.
57. Lehmann U, Heuss ND, McPherson SW, Roehrich H, Gregerson DS. Dendritic cells are early responders to retinal injury. *Neurobiol Dis*. 2010;40:177–184.
58. Wlodarczyk A, Løbner M, Cédile O, Owens T. Comparison of microglia and infiltrating $CD11c^{+}$ cells as antigen presenting cells for T cell proliferation and cytokine response. *J Neuroinflammation*. 2014;11:57.
59. Castanos MV, Zhou DB, Linderman RE, et al. Imaging of macrophage-like cells in living human retina using clinical OCT. *Invest Ophthalmol Vis Sci*. 2020;61:48.
60. Vagaja NN, Chinnery HR, Binz N, Kezic JM, Rakoczy EP, McMenamin PG. Changes in murine hyalocytes are valuable early indicators of ocular disease. *Invest Ophthalmol Vis Sci*. 2012;53:1445–1451.
61. Gloor BP. Mitotic activity in the cortical vitreous cells (hyalocytes) after photocoagulation. *Invest Ophthalmol*. 1969;8:633–646.
62. Wolter JR. Pathology of Henle's fibre layer after occlusion of the central retinal artery. *Br J Ophthalmol*. 1967;51:169–172.

Investigative Ophthalmology & Visual Science